

TEM Study on the Middle Temperature Brittleness of HiSiMo Cast Irons at 400 °C

Wenhui Zhu¹, Larry Godlewski¹, Simon Lekakh², Bitia Ghaffari¹, Carlos Engler-Pinto¹ and Mei Li¹

¹ Research and Innovation Center, Ford Motor Company; Dearborn, MI, USA.

² Missouri University of Science and Technology, Rolla, MO, USA.

High silicon molybdenum (HiSiMo) spheroidal graphite cast irons offer good high-temperature strength and oxidation resistance due to their composition of 4–6 w% silicon and >0.3 w% molybdenum through the formation of a silicon-rich protection layer between the scale/matrix boundary and a cell-like network of Fe₂MoC type eutectic phase at ferrite grain boundaries [1]–[3]. Hence, they are commonly used for high-temperature engine components, such as heat exchangers, and exhaust manifolds [4]–[6]. These components are exposed to thermomechanical fatigue (TMF) loadings due to engine start-stop cycles. Reliable methods to evaluate the TMF properties of the HiSiMo alloys are important to ensure the durability of these components. It is therefore critical to understand the mechanism of the crack initiation and propagation in HiSiMo cast irons. One detrimental feature of HiSiMo cast irons for TMF properties is the middle temperature brittleness (MTB) at ~ 400 °C [7].

This feature has been designated by different authors as elevated temperature brittleness [7]–[9], 673K embrittlement [10], [11], brittleness at medium temperature [12], and intergranular embrittlement [12], [13]. Different mechanisms have been proposed for the MTB phenomenon. Some theories relate the issue to magnesium-assisted sulfur segregation [14] or magnesium segregation [15], depending on the composition of the cast iron. However, it is unknown whether there is any microstructural change causing the MTB. Hence, we designed experiments at different temperatures to validate the MTB and studied the microstructures, based on which we propose a mechanism to explain the MTB of HiSiMo cast irons.

The HiSiMo cast iron bars with the composition listed in Table 1 was casted. Nine tensile samples with a diameter of 6.35 mm and gauge length of 25.4 mm per ASTM D3916 were machined and tensile tested at 300 °C, 400 °C, and 500 °C. The fracture surface morphology and the composition distributions were measured by GEOL 6610 Scanning electron microscopy (SEM) with Energy dispersive X-ray spectroscopy (EDS). Thermo Fisher Scientific Talos transmission electron microscopy (TEM) was employed to examine the fractural surface and the microstructure to elucidate the mechanism for the MTB. The TEM specimens were prepared using a Thermo Fisher Helios G4 PFIB UXe Focused Ion Beam.

The elongation tensile test results of all nine samples, three at each temperature, are shown in Figure 1. The mean values were connected by the lines and the box showing the ranges of the elongation of samples at different temperatures. The elongation to fracture was lowest at 400 °C, about 3% on average. The average strain at 300 °C and 500 °C was about 11% and 5%, respectively. This clearly demonstrated the existence of the MTB at 400 °C. To investigate the root cause for the MTB phenomenon, we examined all fractural surfaces of the tensile bars in detail, selected typical examples of which are shown in Figure 2. Regions with two different features, brittle and ductile fractural regions, were detected in all samples. The EDS results showed no evidence of magnesium segregation, but there were differences in the amount of molybdenum in regions with different morphologies, i.e., there was negligible amounts of Mo in ductile fractural regions, while much more amounts of Mo in the brittle

fractural regions. With this finding, we went further to examine the microstructure by TEM. In Figure 3, the High-angle annular dark-field (HAADF) images demonstrate the differences between samples tested at 400 °C with those at 300 °C and 500 °C by the formation of precipitates at the middle temperature, both in the grain and along the grain boundary. At 400 °C, Mo+Si-containing and Mo-containing precipitates, but not in the samples at the other two temperatures. In addition, we found that some precipitates were carbides, while others were not. The precipitates varied in size and shape, which were either spherical, or rod-like. The precipitation process is a complex transformation relating to temperature, composition, and microstructure. These precipitates may interfere with dislocation movement and harden the alloy, causing the MTB. Interestingly, the precipitation could not be detected from Differential Scanning Calorimetry analysis, possibly due to the small fraction of the precipitates. Further investigation will be conducted on this topic.

In summary, the MTB is a significant issue which needs to be addressed to improve the reliability of HiSiMo cast irons. Here, we used SEM/TEM with EDS to understand the microstructural changes that caused the MTB of HiSiMo cast irons. It was demonstrated that the precipitation occurred reliably at 400 °C but not at either 300°C or 500°C. This work suggests that it is due to the precipitate hardening of the cast irons near 400 °C that these alloys exhibit the MTB phenomenon. Further work needs to be done regarding how to prevent the formation of the precipitates and eliminate the MTB [17].

Alloy	Fe	Si	Mo	C	Cr	Al	Ni	Mn	Mg	Ce	Hf	La	S
HiSiMo	91.3	4.1	0.8	3.2	0.07	0.01	0.2	0.3	0.02	0.01	0.003	0.007	0.006

Table 1. Chemical composition, in wt.%, of the cast iron studied in this work.

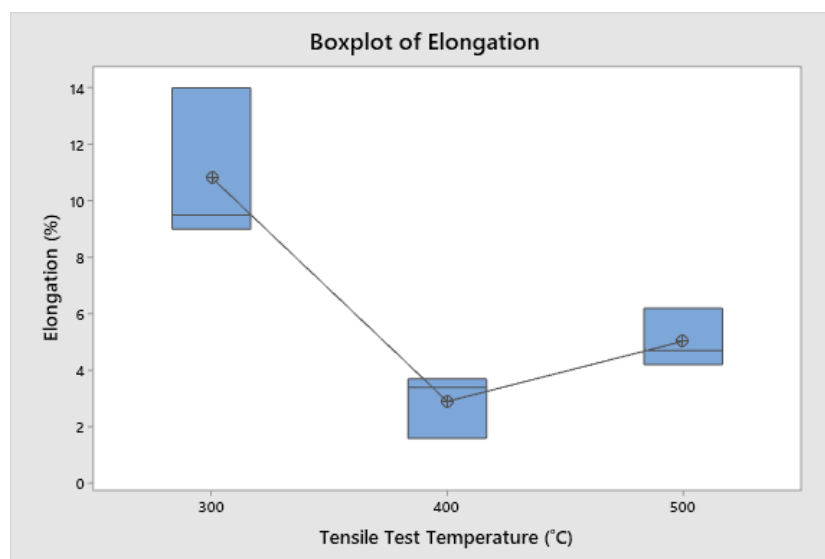


Figure 1. Tensile test results at 300°C, 400°C, and 500°C.

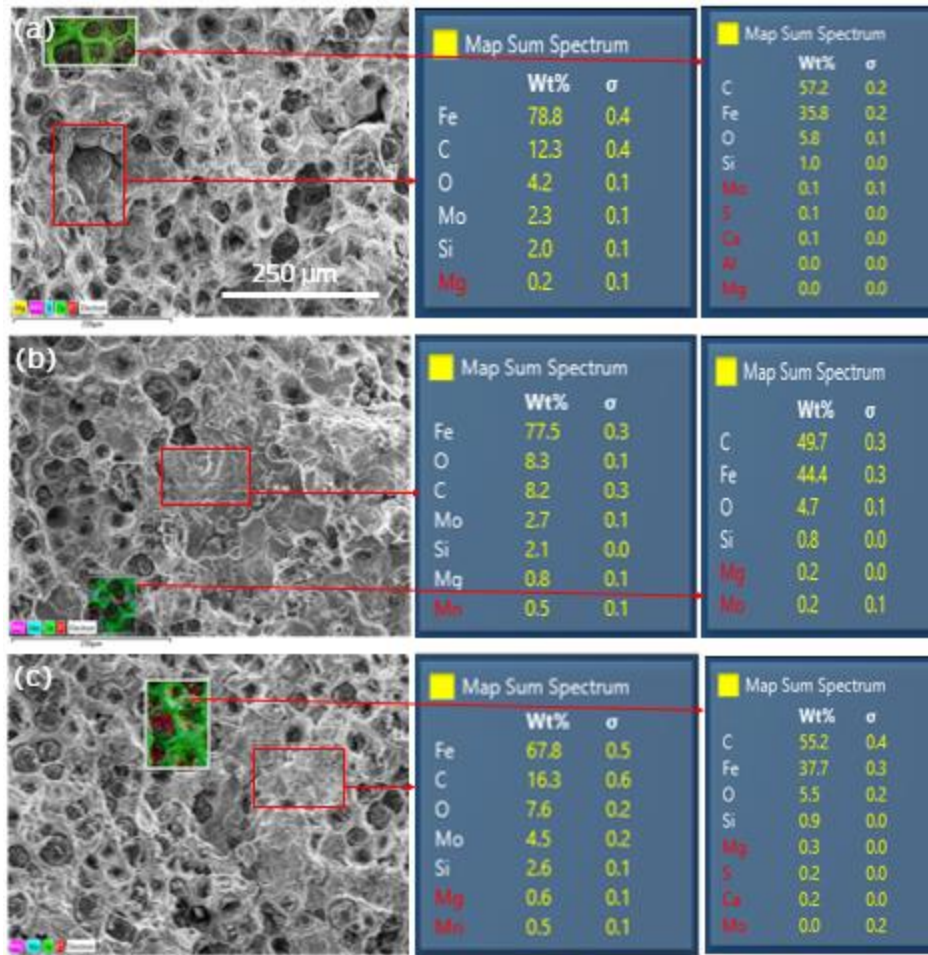


Figure 2. SEM images and EDS results of the brittle and ductile fracture regions on typical fracture surfaces of the tensile bars after the tensile tests at different temperatures. (a) 300°C, (b) 400°C, and (c) 500°C. The scale bar is 250 μm.

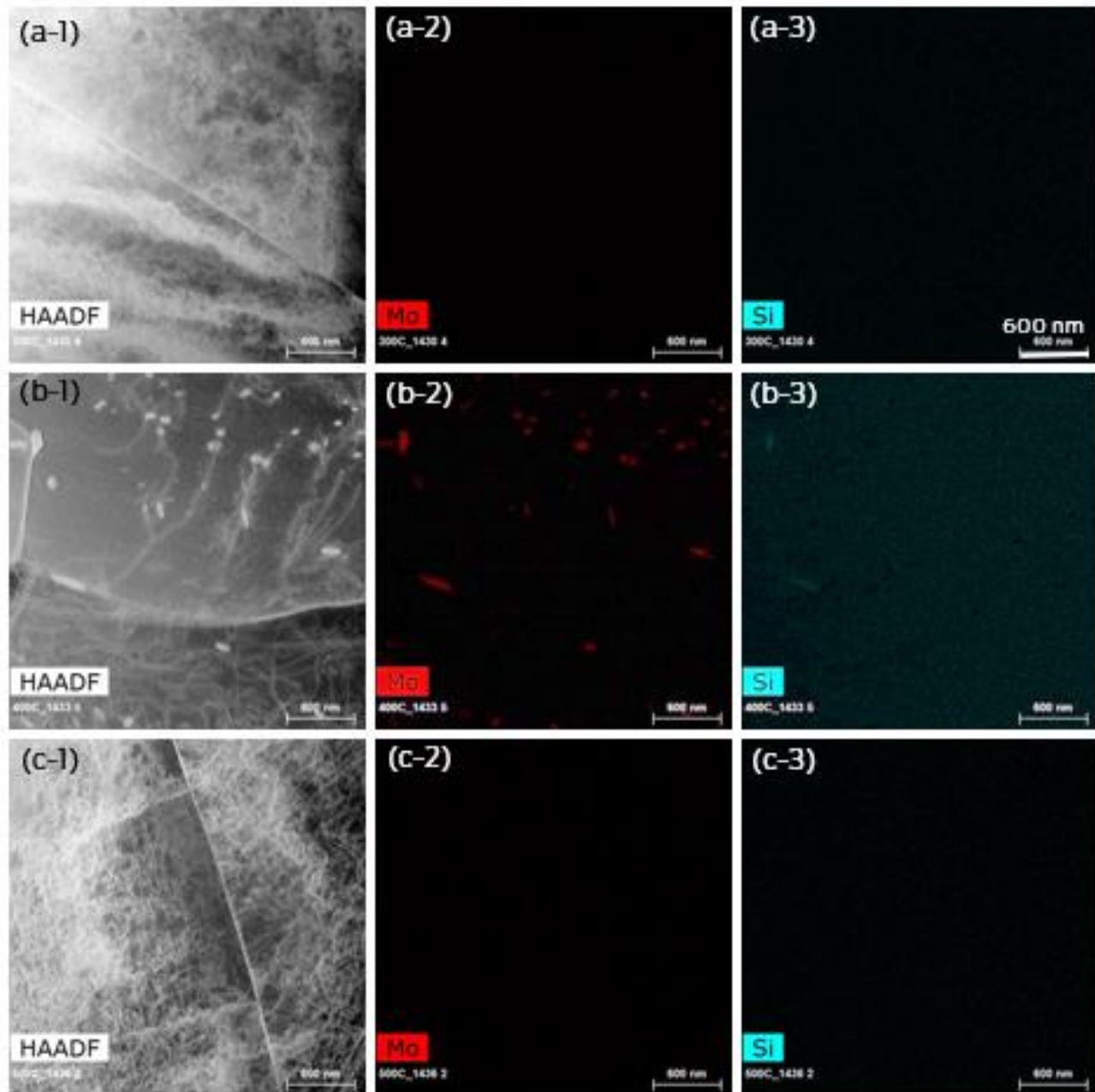


Figure 3. TEM images and EDS results of tensile samples tested at (a) 300°C, (b) 400°C, and (c) 500°C. Precipitates containing Mo, with and without Si and both along the grain boundaries and within the grains, were only formed at 400°C. The scale bar is 600 nm.

References:

- [1] H. Guo, W. Jia, and F. Ahdad, “Modeling and Simulation of Tube with HiSiMo Ductile Iron under High Speed Impact,” (SAE International, Warrendale) SAE Technical Paper. doi: 10.4271/2018-01-0097.
- [2] S. H. Park et al., “Development of a Heat Resistant Cast Iron Alloy for Engine Exhaust Manifolds,” (2005), p. 2005-01–1688. doi: 10.4271/2005-01-1688

- [3] D. Li et al., “Solidification Behavior, Microstructure, Mechanical Properties, Hot Oxidation and Thermal Fatigue Resistance of High Silicon SiMo Nodular Cast Irons,” (2004), p. 2004-01–0792. doi: 10.4271/2004-01-0792
- [4] X. Wang et al., *Metals* (**9**, **6**), 6. doi: 10.3390/met9060648
- [5] K. Avery, J. Pan, and C. Engler-Pinto, “Effect of Temperature Cycle on Thermomechanical Fatigue Life of a High Silicon Molybdenum Ductile Cast Iron,” SAE Technical Paper (2015).
- [6] E. G. Trelles and C. Schweizer, *Int. J. Fatigue* (**155**), p. 106592. doi: 10.1016/j.ijfatigue.2021.106592
- [7] L. Delin et al., *SAE Trans.* (**116**) (2007), p. 530.
- [8] R. N. Wright and T. R. Farrell, *AFS Trans* **93** (1985), p. 853.
- [9] “Prevention of Elevated Temperature Brittleness in Ferritic Ductile Iron by Phosphorus,” https://www.jstage.jst.go.jp/article/jfes/69/4/69_4_304/_article (accessed Nov. 30, 2021).
- [10] O. Yanagisawa and T. S. Lui, *Trans. Jpn. Inst. Met.* **24** (1983), 12, p. 858. doi: 10.2320/matertrans1960.24.858
- [11] H. Borgström, *Minerals* (**11**, **4**), 4 (2021). doi: 10.3390/min11040391
- [12] E. G. Trelles, S. Eckmann, and C. Schweizer, *Int. J. Fatigue* **155** (2022), p. 106573. doi: 10.1016/j.ijfatigue.2021.106573
- [13] X. Wu et al., *Metall. Mater. Trans. A* **45**, 11 (2014), p. 5085. doi: 10.1007/s11661-014-2468-x
- [14] R. N. Wright and T. R. Farrell, *AFS Trans* **93** (1985), p. 853.
- [15] K. R. Avery, “A Predictive Framework for Thermomechanical Fatigue Life of High Silicon Molybdenum Ductile Cast Iron Based on Considerations of Strain Energy Dissipation,” <https://ui.adsabs.harvard.edu/abs/2016PhDT.....74A> (Accessed Nov. 30, 2021).
- [16] S. N. Lekakh et al., *Metall. Mater. Trans. B* **51**, 6 (2020), p. 2542. doi: 10.1007/s11663-020-01975-w
- [17] The authors would like to thank the financial support by the U.S. Department of Energy, Office of Energy Efficiency and Renewable Energy (Vehicle Technologies Office, Propulsion Materials Program) under Award No. DE-EE0008458.